

## Variation of nuclear level density parameter as function of excitation energy

G. K. Prajapati<sup>1,\*</sup>, Y. K. Gupta<sup>1</sup>, B. N. Joshi<sup>1</sup>, L. S. Danu<sup>1</sup>, N. Kumar<sup>1</sup>, S. Dubey<sup>1,2</sup>, S. Mukhopadhyay<sup>1</sup>, R. P. Vind<sup>1</sup>, B. John<sup>1</sup>, and D. C. Biswas<sup>1</sup>

<sup>1</sup>Nuclear Physics Division, Bhabha Atomic Research Centre, Mumbai - 400085, INDIA and

<sup>2</sup>Physics Department, The M. S. University of Baroda, Vadodara-390002, INDIA

### Introduction

Nuclear level density (NLD) parameter,  $a$ , is of fundamental importance and its precise value is needed for applied research as well. It is a key ingredient in the prediction of reaction cross sections using statistical model codes [1]. Assuming equidistant Fermi Gas Model (FGM) for non interacting fermions, the most widely used expression for the NLD is given as;

$$\rho(U) = \frac{\sqrt{\pi} \exp(2\sqrt{aU})}{12 a^{1/4} U^{5/4}} \quad (1)$$

where  $U$  is the excitation energy of the nucleus. In the above model, the parameter  $a$  is constant for a given nucleus as,  $a = \frac{\pi^2 g}{6}$ , where  $g$  is the single particle level density around the Fermi energy. Within this phenomenological framework, the FGM yields  $a = A/15$ , however, experimental value at excitation energy below 10 MeV is about  $A/8 \text{ MeV}^{-1}$ . This difference have been understood in terms of finite nuclear size and nucleon effective mass.

It has been of continued research interest to investigate the transition of the level density parameter,  $a$ , from very low to high excitation energies. The experimental information at higher excitation energies on the parameter  $a$  comes from evaporation spectra of excited nucleus. It has been reported in many cases that the parameter  $a$  deviates from its liquid drop value of  $A/8 \text{ MeV}^{-1}$  and approaches to FGM value of  $A/15 \text{ MeV}^{-1}$  with increasing excitation energy [2, 3]. Study of transition pattern from liquid drop to FGM value has to be explored in different mass regions. In the present work, we report the behavior of NLD parameter as function of excitation energy around mass region around 112 measured through  $\alpha$ -particle evaporation spectra

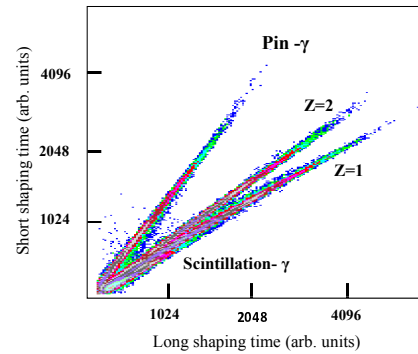


FIG. 1: Typical long vs short shaping time graph for  $^{16}\text{O}+^{100}\text{Mo}$  system at 75 MeV.

in  $^{16}\text{O}+^{100}\text{Mo}$  reaction.

### Experimental Details and Data Analysis

The experiment was performed using  $^{16}\text{O}$  beam from BARC-TIFR Pelletron facility, Mumbai, India. A self supporting foil of  $^{100}\text{Mo}$  ( $1.0 \text{ mg/cm}^2$ ) was used as the target. Measurements were performed at beam energies  $E_{Lab} = 55, 60, 70, 75,$  and  $80 \text{ MeV}$  which leads to excitation energies in the range of 46-70 MeV in compound nucleus (CN),  $^{116}\text{Sn}$ . The charge particles evaporated in the backward hemisphere were detected using five CsI(Tl) detectors of 10 mm thickness. CsI(Tl) detectors were mounted at  $124^\circ, 134^\circ, 145^\circ, 150^\circ,$  and  $155^\circ$  with respect to beam direction. Two silicon surface barrier detector having solid angles of  $\sim 0.30 \text{ msr}$  were placed at  $\pm 20^\circ$  for Rutherford normalization purpose. Ballistic deficit technique [4] for CsI(Tl) detectors was used for particle identification by employing two shaping amplifiers, one with short shaping time ( $0.2 \mu\text{s}$ ) and the other with long shaping time ( $3.0 \mu\text{s}$ ). Fig. 1 shows a two-dimensional plot of short versus long shaping time pulse heights. One can see from Fig. 1 that  $\alpha$  particles are clearly separated among others. The

*Available online at [www.symprp.org/proceedings](http://www.symprp.org/proceedings)*

\*Electronic address: [shyam@barc.gov.in](mailto:shyam@barc.gov.in)

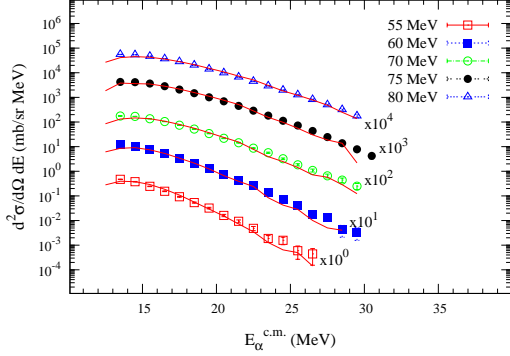


FIG. 2: Experimental  $\alpha$  particle energy spectra of different excitation energies along with PACE2 calculations for  $^{16}\text{O}+^{100}\text{Mo}$  system.

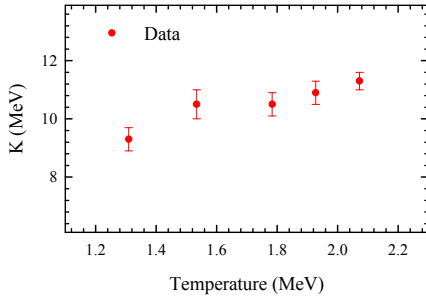


FIG. 3: Inverse level density parameter ( $K$ ) as a function of temperature.

CsI(Tl) detectors were energy calibrated using  $^{228,229}\text{Th}$   $\alpha$  sources. Extrapolation of the light yield produced in CsI(Tl) detectors beyond 8 MeV was performed using in-beam data from earlier measurements [5, 6].

The measured  $\alpha$  particle energy spectra at different angles were converted to centre-of-mass frame using the standard Jacobian. The c.m. spectra of different laboratory angles overlapped very well, indicating dominant compound nuclear evaporation.

## Results and Discussions

Averaged c.m. spectra were compared with statistical model code PACE2 predictions. The diffuseness parameter was chosen to be  $0.5 \hbar$ . The inverse level density parameter  $K = A/a$  was kept as free parameter to obtain a best fit using  $\chi^2$  minimization technique. Data were fitted in the  $\alpha$  particle energy range

of 14.5-30 MeV. The PACE2 calculations corresponding to the best fit are shown in Fig. 2 for different beam energies. The spectra in the Fig.2 are scaled to suitable factors for better visualization. The best fitted inverse level density parameter thus determined is presented in the Table I. Temperature of the residual nucleus was determined using the relation,  $T = \sqrt{\frac{U}{a}}$ , where  $U = E_{CN}^* - E_k^\alpha - S_\alpha$ .  $E_{CN}^*$ ,  $E_k^\alpha$ , and  $S_\alpha$  are the initial compound nucleus excitation energy, kinetic energy of the  $\alpha$  particle, and  $\alpha$  particle separation energy, respectively. It is observed from Fig. 3 that the parameter  $K$  increases almost linearly with the temperature. Present data follow the similar trend as reported earlier in the mass region of  $A=160$  [7]. These results are preliminary and detailed results would be presented.

TABLE I: Relevant experimental parameter studied for  $^{16}\text{O}+^{100}\text{Mo}$  system.

$E_{Lab}$ (MeV)	$E_{CN}^*$ (MeV)	U (MeV)	K (MeV)	T (MeV)
55	46.28	20.66	$9.3 \pm 0.4$	1.30
60	50.74	25.12	$10.5 \pm 0.4$	1.53
70	59.47	33.85	$10.5 \pm 0.5$	1.78
75	63.84	38.22	$10.9 \pm 0.4$	1.92
80	68.20	42.58	$11.3 \pm 0.3$	2.07

## Acknowledgments

We are thankful to BARC-TIFR pelletron staff for smooth running of the machine during experiment.

## References

- [1] H. A. Bethe Phys. Rev. **50**, 332 (1936).
- [2] B. J. Fineman *et al.*, Phys. Rev. C **50**, 1991 (1994).
- [3] D. Febris *et al.*, Phys. Rev. C **50**, 1261(R) (1994).
- [4] J. Gal *et al.*, Nuclear Instruments and methods in Physics Research A **366**, 120 (1995).
- [5] Y. K. Gupta *et al.*, Phys. Rev. C **84**, 031603 (2011).
- [6] Y. K. Gupta *et al.*, Phys. Rev. C **86**, 01461502 (2012).
- [7] G. Nebbia *et al.*, Phys. Lett. B **176**, 20 (1986).